JOURNAL OF THE KOREAN ASTRONOMICAL SOCIETY
29: 223~243, 1996

THE SWINGS EFFECTS OF THE A-X SYSTEM AND v" = 1-0 BAND OF CO

KIM, SANG -JOON
Kyung Hee Observatory, Institute of Natural Sciences
Department of Astronomy and Space Science, Kyung Hee University, Suwon, KOREA
e-mail:sjkim@khobs.kyunghee.ac.kr
(Received September 13, 1996; Accepted October 15, 1996)

ABSTRACT

We have constructed a line-by-line model of the A-X system of CO in order to analyze the CO bands appearing in the UV spectra of comets. The model includes electronic, rotational, vibrational transitions, excitations by solar UV radiation, and effects of neutral and electron collisions. The major bands of the A-X system occur in the 1200 - 1800 $\AA$ range where the temporal variation of solar irradiation is significant. The solar spectrum in this spectral range shows many emission lines, which cause a significant Swings effect. We derived fluorescence efficiencies of the bands as functions of heliocentric velocity and cometocentric distance using a high resolution spectrum of the sun. We compared our model with a spectrum of comet P/Halley obtained with the IUE, and estimated that the UV Swings effects are less than 20 fluorescence efficiencies for the most bands of the A-X system. We discuss the temporal variation of solar UV irradiation and its effects on the fluorescence efficiencies. The study of the A-X system also requires knowledge of vibrational and rotational fluorescent processes in the infrared and radio regions because the majority of CO molecules in the coma is in the ground rotational states. The solar infrared spectrum near 5 microns, where the fundamental band of CO occurs, contains strong absorption lines of the fundamental band and hot bands of CO and its isotopes. We derived fluorescence efficiencies of the infrared band as functions of heliocentric velocity and cometrocentric distance. The solar absorption lines near 5 microns cause a 20 reduction of the g-factor of the fundamental band at heliocentric velocities close to 0 km/sec. We discuss the effects of neutral and electron collisions on the fluorescence efficiencies of the infrared and UV bands.

Key Words : comet, coma, molecule

I. INTRODUCTION

CO is probably the second most abundant constituent next to H_2O in cometary comae. The major electronic band, the A-X system, is located in the 1200 - 1800 $\AA$ range where solar irradiation is very low, and therefore its fluorescence efficiency is very low. The weak and noisy A-X bands among strong cometary atomic lines have been seen in UV spectra taken with the International Ultraviolet Explorer (IUE) (e.g., Festou, et al. 1986), the Hubble Space Telescope (HST) (Weaver et al. 1992), and rockets (e.g., Feldman, 1982). Weaver, et al. (1992) reported a detection of the Cameron band in emission between 1800 - 2400 $\AA$ in the spectra of comets Shoemaker & Levy (1991a1) and Hartley obtained by the Faint Object Spectrometer (FOS) on the HST. Recently, high signal-to-noise (S/N) spectra of the A-X bands of comet Hyakutake (1996B2) have been obtained with the HST, but the CO lines have been mostly saturated (Weaver, private communication, 1996). On the other hand, the detection of ro-vibrational lines of the v"=1 $\rightarrow$ 0 band through the 5 micron atmospheric window has been difficult. Disanti et al. (1992) reported a tentative detection of the P(3) of the v=1-0 band in comet Austin (1990 V), but they did not find the P(2) line in the same spectra.

Durrance (1980) calculated the g-factors of the A-X bands. He used a single-cycle fluorescence for the calculations of the g-factors including v' =0 to 12 in the A state and only v"=0 state in the X state. For an approximate calculation, he did not inclinclude vibrational spontaneous deexcitations and vibrational excitations by solar infrared radiation in the X state. He did not consider Swings effects caused by numerous emission lines in the solar UV spectrum, although he considered the effects for a few specific CO lines. For rotational levels in the v"=0 state, he assumed a Boltzmann distribution, which turn out to be a very rough approximation according to calculations done by Chin and Weaver (1984).

Chin and Weaver performed time-dependent fluorescence calculations assuming CO being only produced from cometary nucleus. Eberhardt, et al. (1987) reported that the almost same amount of CO can also be produced by an extended source, such as the "CHON" particles, in the inner coma of P/Halley based on data from the Neutral Gas Mass Spectrometer (NMS) onboard Giotto. The emission of the A-X bands of CO was observed far from nucleus because of its long lifetime (10^6 seconds) against photodissociation by solar UV. Recently Sahnow, et al. (1993) presented spatial intensity distributions of the A-X bands in comet Austin (1990 V), which was observed by a rocket, but they found no evidence of the extended source for CO probably because of a low dust-gas ratio in this comet. Chin and Weaver constructed their infrared model including excitations by H_2O collisions, considering only v" = 0 and 1 levels in the X state, and including pure rotational transitions , but ignoring UV transitions and without considering inf rared Swings effects. Crovisier and Le Bourlot (1983) and Billebaud et al. (1991) constructed fluorescence band models of the v"=1→ 0 transition for comets and Mars, respectively, but they did not include the Swings effects in their models.

In this paper, we unify the infrared and UV models of Chin and Weaver (1984) and Durrance (1980), respectively, including effects they ignored, using updated information, and considering fluorescent equilibrium for certain transitions. The unified model includes: (1) updated high-resolution solar UV spectrum for proper calculations of the Swings effects; (2) ATMOS (Atmospheric Trace Molecule Spectroscopy) solar infrared spectrum containing strong absorption lines of the fundamental bands and the hot bands of CO and its isotopes; (3) pure rotational excitations and deexcitations by electron collisions, which are found to be important for diatomic molecules having a dipole moment (Kim, A'Hearn, and Cochran, 1989); (4) updated pure rotational excitation and deexcitation rates by H_2O collisions (S. Green, private communications, 1992); and (5) pure rotational transitions up to j"=29, pure ro-vibrational transitions up to v"=15 in the X state, and electronic transitions up to v'=12 in the A state. The solar absorption and emission lines in the infrared and UV ranges, respectively, cause significant Swings effects. We derive fluorescence efficiencies of the infrared and UV bands and calculate infrared and UV Swings effects. We present comparisons of our models and an IUE Halley spectrum.

II. OBSERVATIONS

We prepared IUE comet spectra, which cover the shorter wavelength range (1100 - 1800 $\AA$). An extensive IUE comet spectra have been archived at the Astronomy Department of the University of Maryland since early 1980s. We found 5 comet P/Halley spectra, 1 comet Wilson (1987 VI) spectrum, and 2 comet Levy (1990c) spectra, which have good S/N ratios showing discernable structures of the CO A-X system. Among these spectra, we chose the best S/N spectrum, which is a comet Halley spectrum (SWP27908) taken on March 13/14, 1986 near the Giotto and Vega encounter times with the comet. This spectrum is very useful, because *In situ* data obtained from the spacecraft for neutral and ion densities as a function of cometocentric velocity are important information for the investigation of the effects of neutral and ion collisions on the CO fluorescence process. The heliocentric and geocentric distances, and the heliocentric velocity at the time of the IUE observations were 0.9 and 1.0 AU, and 34.6 km/sec, respective ly. The total exposure time was 70 minutes. The size of the IUE object slit was 140 square arcsec (9.3 arcsec × 15.1 arcsec) consisting 110 rows. We obtained an object spectrum from spectra in row numbers from 48 to 61, and used spectra in row numbers from 30 to 39 and from 70 to 79 for background subtraction. Some of the IUE spectra of comet P/Halley taken from March 9 to 16, 1986 were previoulsy published in Festou et al. (1986).

III. MODELING

We consider rotational, ro-vibrational, and electronic transitions in order to construct a model, which includes fluorescence and collision effects. In the following sections (1), (2), and (3), various parameters involved in these transitions are described in detail. In the section (4) we present fluorescence calculations and g-factors.

(a) Rotational Transitions

Term values, quantum numbers, weights, and line positions of the pure rotational transitions in the X state were adopted from an updated radio line catalog compiled by Poynter and Pickett (1992). The data are in a digital form, and they were obtained from the Jet Propulsion Laboratory through network in 1992. A hard copy document was published in 1984 by Poynter and Pickett, but the data are supposed to be the most updated. Einstein A coefficients for fluorescence modelings were calculated using Eq. (6) in the 1984 hardcopy document of Poynter and Pickett.

The Einstein A coefficients range from 7.16×10^{-8} to 8.32×10^{-4} sec^{-1} for rotational quantum number j" = 1 to 20, respectively. These values are orders of magnitude lower than those of other comentary diatomic molecules such as OH, CH, NH, etc. The low Einstein A coefficients are due to the low dipole moment (0.1 Debyes) of CO, compared with those (1 2 Debyes) of the above diatomic molecules. Rotational excitation rates by solar radiation or cosmic background 3 K radiation are even smaller than the Einstein A coefficients, and much smaller than the excitation rates by H_2O or electron collisions, which will be discussed below. We therefore ignore these excitation rates.

For the rates of rotational excitation and deexcitation by H_2O collisions, we adopted a computer program and updated theoretical values provided by S. Green (private communication, 1992). He constructed the model based on his extensive experience in collisional rate calculations for N_2-H_2O system. The computer program has been used for the calculations of the rates as a function of tempearture. We adopted a temperature profile of Crifo (1992; and private communcations, 1993) for a Halley type comet near 1 AU. We present the rates in Table 1 for Δ j" = 1 transitions of CO in a 200 K Boltzmann distribution of H_2O molecules. For a Halley type comet, the excitation rates for Δ j" = 1 at 1 AU are about 1×10^{-4} sec^{-1} and 1×10^{-8} sec^{-1} at 10^4 km and 10^6 km from the nucleus, respectively. Here we adopted Figure 4 of Kim et al. (1989) for neutral (mostly H_2O) and ion density curves observed by Vega and Giotto spacecraft for Halley at 1 AU. The ion density will be used for an electron density assuming overall charge neutrality, and it will be used for the calculations of excitation rates by electrons in the next paragraph. For Δ j" $\neq$ 1, the CO-H_2O excitation rates are less than those of the Δ j" = 1, but we include these transitions. The deexcitation rates are in the same order of magnitude as excitation rates at 200 K. Chin and Weaver (1984) used old rates provided by S. Green at that time. The old rates for the Δ j" = 1 are about a factor of 5 times higher than the new values for j" = 1, and about a factor of 2 times higher than the new values for j" ¿ 5.

Rotational excitations and deexcitations by electron collisions are found to be important processes for diatomic polar molecules in outer regions of cometary comae, where electron density becomes comparable with neutral density (Kim, et al. 1989). We used Eqs. (1) and (2) of Dickinson et al. (1977) for the calculations of the excitation rates for the Δ j" = 1 transitions. Deexcitation rates have been obtained by detailed balancing. The excitation rates are very slowly dependent on electron temperature when it is greater than 1000 K. We used an electron temperature range of 5,000 - 10,000 K derived from the results of Vega 1 and 2 encounters with comet P/Halley (Pedersen, et al. 1987). For a Halley type comet, the excitation rates at 1 AU are about 3×10^{-5} sec^{-1} and 3×10^{-7} sec^{-1} at 10^4 km and 10^6 km from the nucleus, respectively. For the electron temperature range of 5,000 - 10,000 K, we adopted excitation cross sections for j" = 0 $\rightarrow$1, 0 $\rightarrow$ 2, 0 $\rightarrow$ 3, 0 $\rightarrow$ 4, 1 $\rightarrow$ 2, 1 $\rightarrow$ 3, 1 $\rightarrow$ 4, and 1 $\rightarrow$ 5 transitions listed in Tables 4 and 6 of Chandra (1977), and extrapolate these values to other higher transitions. For Δ j" $\neq$ 1, the rates are substantially less than those of Δ j" = 1 in general as demonstrated in Chandra (1977) and Jain and Norcross (1992), and therefore the above extrapolation does not cause siginificant uncertainty in our model. Within the above temperature range, the deexcitation rates are virtually the same as the excitation rates.

From the above consideration for various rates, it is clear that in the inner coma regions (¡ 10^4 km from the nucleus) rotational excitations by H_2O collisions dominate over electron and radiative excitations. In the outer coma regions (¿ 10^5 km from the nucleus) electron excitations become important. These rates along with other rates, which will be presented below, are summarized in Table 2.

Table 1. Rotational transition rates (cm^3 sec) of CO for Δ j" = 1 by H_2O collisions at 200 K. j_{int} and j_{fin} are initial and final rotational states, respectively.

j_{int}	j_{fin}	$cm^3 sec$	j_{int}	j_{fin}	$cm^3 sec$
0	1	0.143E-09	15	14	0.739E-10
1	0	0.490E-10	15	16	0.461E-10
1	2	0.151E-09	16	15	0.675E-10
2	1	0.955E-10	16	17	0.407E-10
2	3	0.162E-09	17	16	0.614E-10
3	2	0.126E-09	17	18	0.358E-10
3	4	0.161E-09	18	17	0.558E-10
4	3	0.140E-09	18	19	0.314E-10
4	5	0.152E-09	19	18	0.505E-10
5	4	0.142E-09	19	20	0.275E-10
5	6	0.140E-09	20	19	0.455E-10
6	5	0.139E-09	20	21	0.240E-10
6	7	0.127E-09	21	20	0.410E-10
7	6	0.134E-09	21	22	0.210E-10
7	8	0.115E-09	22	21	0.368E-10
8	7	0.126E-09	22	23	0.182E-10
8	9	0.103E-09	23	22	0.330E-10
9	8	0.119E-09	23	24	0.158E-10
9	10	0.929E-10	24	23	0.295E-10
10	9	0.111E-09	24	25	0.137E-10
10	11	0.832E-10	25	24	0.263E-10
11	10	0.103E-09	25	26	0.119E-10
11	12	0.743E-10	26	25	0.234E-10
12	11	0.953E-10	26	27	0.102E-10
12	13	0.662E-10	27	26	0.208E-10
13	12	0.878E-10	27	28	0.883E-10
13	14	0.589E-10	28	27	0.185E-10
14	13	0.807E-10	28	29	0.761E-10
14	15	0.522E-10	29	28	0.164E-10

(b) Ro-Vibrational Transitions

Line positions, term values, ro-vibrational quantum numbers, and line intensities for v" = 1-0, 2-0, 2-1, 3-0 transitions were adopted from the HITRAN (High-resolution Transmission Molecular Absorption Database) 1992. The HITRAN line list is the most updated data for the ro-vibrational bands of CO. Einstein A coefficients (A) for these transitions were calculated from the line intensities. Einstein A coefficients for other higher Δ v"=1 transitions were calculated from ratios of A(v $\rightarrow$ v-1) and A(1 $\rightarrow$ 0) presented in Table 2 of Djeu and Searles (1972). They presented the ratios up to v"=12. We were able to e xtrapolate their ratios up to v"=25, because the ratio varies smoothly as a function of v". We found that A(1 $\rightarrow$ 0) is about 30 sec^{-1}, and A(25 $\rightarrow$ 24) is about 320 sec^{-1}. Einstein A coefficients for Δ v" = 2 transitions are only several percents of Δ v" =1 transitions according to Roux et al. (1972) and Legay-Sommaire and Legay (1970). We therefore ignored Δ v" = 2 transitions except v" = 2 $\rightarrow$ 0 transition. Δ v" = 3 transitions are even weaker than Δ v" = 2 transitions, and therefore we ignored Δ v" = 3 transitions except v" = 3 $\rightarrow$ 0 transition.

Excitation by solar infrared radiation is significant. In fact the infrared excitation rates for the Δ v" =1 transitions

Table 2. Various excitation and deexcitation rates at ρ=10^3, 10^4, and 10^5 km at 1 AU for a Halley type comet.

Transition	Rate(sec^{-1}) $\rho = 10^3$km	10^4km	10^5km
Rotational spontaneous deexcitation from j" = 1 → 0	7.16×10^{-8}	7.16×10^{-8}	7.16×10^{-8}
Rotational spontaneous deexcitation from j" = 20 → 19	8.32×10^{-4}	8.32×10^{-4}	8.32×10^{-4}
Rotational transition rates (j"=0 → 1) by H_2O collisions at 200 K.	1×10^{-3}	1×10^{-4}	1×10^{-6}
Rotational transition rates (j"=1 → 0) by H_2O collisions at 200 K.	5×10^{-4}	5×10^{-5}	5×10^{-7}
Rotational transition rates (j"=0 → 1) by electron collisions.	3×10^{-4}	3×10^{-5}	1×10^{-6}
Rotational transition rates (j"=1 → 0) by electron collisions.	3×10^{-4}	3×10^{-5}	1×10^{-6}
Vibrational Spontaneous transition rates (v"=1 → 0)	30	30	30
Vibrational Spontaneous transition rates (v"=25 → 24)	320	320	320
Vibrational excitation by solar infrared radiation (v"=0 → 1)	2×10^{-4}	2×10^{-4}	2×10^{-4}
Vibrational excitation by solar infrared radiation (v"=0 → 2)	3×10^{-6}	3×10^{-6}	3×10^{-6}
Vibrational excitation by solar infrared radiation (v"=0 → 3)	2×10^{-8}	2×10^{-8}	2×10^{-4}
Electronic excitation by solar UV radiation (v"=0 → v'=1)	4×10^{-7}	4×10^{-7}	4×10^{-7}

turn out to be greater than the rotational excitation rates presented above, and electronic excitation (X → A) rates which are usually several times of 10^{-7} sec^{-1} for strong bands. The v" = 0 → 1 excitation rate is about 2 × 10^{-4} sec^{-1}, and rates are even higher for high Δ v" =1 transitions. For v"= 0 → 2 and 0 → 3 rates, we found approximately 3 × $10^{-6}$$sec^{-1}$ and 2 × 10^{-8} sec^{-1}, respectively.

To our knowledge, vibrational deexcitation rates of CO by H_2O or OH collisions are not available in the literature, although some works had been done for CO-CH_4 (Abdel-Halim, and Ewing, 1985), CO-He (Boissoles, et al., 1989), CO-H_2 (Bacic, et al. 1985), CO-HCl (Vlahoyannis, et al. 1987), and CO-H collisions (Lee and Bowman, 1987). The vibrational deexcitation rates for CO-He and CO-H_2 collisions at 200 K are 3×10^{-18} cm^3 sec^{-1}, and 2×10^{-16} cm^3 sec^{-1}, respectively. Assuming that the CO-H_2O rate is the same as these values and the H_2O density at cometary surface is $10^{12} cm^{-3}$, the deexcitation rates are 3×10^{-6} sec^{-1} or 2×10^{-4} sec^{-1}, which is negligible compared with A(v"=1 $\rightarrow$ 0) 30 sec^{-1}. On the other hand, we performed a rough calculation using a method given by Schwartz et al. (1952), and found 3×10^{-16} cm^3 sec^{-1} and therefore 3×10^{-4} sec^{-1} for the CO-H_2O rate at the nucleus surface, and smaller values for the CO-OH rate. We however caution readers that this method causes 1 - 2 orders of magnitude uncertainty. The rates are nevertheless comfortably less than the A(v"=1 $\rightarrow$ 0) 30 sec^{-1}, after the uncertainty is considered. Excitation rates are also negligible compared with other ro-vibrational excitations discussed above, because the rates are determined by the detailed balancing equation, which contains a Boltzmann factor of 10^{-7} at 200 K. In this work, we therefore neglect vibrational excitations and deexcitations by collisions.

(c) Electronic Transitions

Tilford and Simmons (1972) compiled works published by several authors before 1972 and presented various molecular band constants, an energy diagram, observed absorption lines of the A-X, B-X, C-X, and D-X transitions, and band origins of these transitions plus eight forbidden transitions. The observed A-X bands in cometary spectra span from 1200 to 1800 A. The B-X, C-X, D-X systems occur shorter wavelength ranges, where solar UV radiation rapidly decreases, and their influence on the A-X band is minimal. We therefore neglect these transitions along with the forbidden transitions. We also neglect the B-A system, because of the same reason, i.e., X $\rightarrow$ B and subsequent B $\rightarrow$ A transition rates are negligible compared with X $\rightarrow$ A transition rates. This greatly simplifies the model calculations and makes the calculations realistic because the number of lines included in A-X m odel alone is about 20,000.

The $A^1\Pi$ - $X^1\Sigma$ transitions give rise P, Q, and R baranches. In the A state the rotational quantum number j' starts from 1 instead of 0. This causes that P, Q, and R branches start from j" = 2, 1, and 0, respectively, in X state. Tilford and Simmons (1972) present a line list only for v" = 0 $\rightarrow$ v' = 0-20 transitions. We calculated lines for v" = 0-15 $\rightarrow$ v'= 0-12 transitions using molecular constants in the tables of Tilford and Simmons, and found the discrepancy for unperturbed lines is mostly less than 0.05 A, which is satisfactory for our modeling purpose.

A complication in the modeling arises from significant perturbation at rotational energy levels in the A state. The perturbation is caused by overlapping of the A state potential curve with other electronic potential curves. We estimate from the line list of Tilford and Simmons that about 10 all the v" = 0 $\rightarrow$ v' = 0-20 transitions are perturbed. In our model we do not included perturbed lines for the v" = 1 $\rightarrow$ v' = 0-12 transitions, because we do not have laboratory observation about these perturbed line positions. We estimate that the uncertainty from this simplification causes less than 3 the CO lines are highly accumulated, the effect on the g-factor due to the misplacement of the perturbed lines is roughly canceled out.

Between the late 1960s and early 1970s, there were discussions among laboratory chemists that oscillator strengths derived from radiative lifetimes (e.g., Hesser, 1968) are about a factor of two less than those derived from electron impact experiments (e.g., Lassettre and Skerbele, 1971). Mumma et al. (1971) deduced a transition moment with a linear dependence on the internuclear distance (r) from their own emission intensity measurements. Mumma et al. found that the use of this transition moment reduces the factor of disagreement from 2 to 1.3. We adopted Einstein A coefficients of Mumma et al., who provided the values up to v'=9 and v"=12.

Einstein A coefficients ($A_{v'v"}$) for vibrational transitions are given by:

$$A_{v'v"} = A_{v'} \frac{q_{v'v"} Re^2(r_{v'v"}) \lambda^{-3}_{v'v"}}{\Sigma_{v"} q_{v'v"} Re^2(r_{v'v"}) \lambda^{-3}_{v'v"}} \quad (1)$$

where $q_{v'v"}$ is the Franck-Condon factors, $Re(r_{v'v"})$ is the transition moment, $r_{v'v"}$ is the internuclear distance, and $\lambda_{v'v"}$ is the band head wavelength. $A_{v'}$ is defined as:

$$A_{v'} \equiv \frac{1}{\tau_{v'}} = \Sigma_{v"} A'_v v" \tag{2a}$$

where $\tau_{v'}$ is the radiative lifetime at v' level. The branching ratio b is defined by:

$$b_{v'v"} \equiv \frac{A_{v'v"}}{A_{v'}} = \frac{q_{v'v"} Re^2(r_{v'v"}) \lambda^{-3}_{v'v"}}{\Sigma_{v"} q_{v'v"} Re^2(r_{v'v"}) \lambda^{-3}_{v'v"}} \tag{2b}$$

The oscillator strength is related with the $A_{v'v"}$, as follows:

$$f_{v'v"} = 1.499 \frac{(2 - \Delta_{0,\lambda'})}{(2 - \Delta_{0,\lambda"})} \frac{1}{\omega^2_{v'v"}} A_{v'v"} \tag{3}$$

which was taken from Table 4 of Larsson (1983). Here $\omega_{v'v"}$ is the band head wavenumber, and $\lambda' = 1$ and $\lambda" = 0$ for the $A^1\Pi - X^1\Sigma$ system.

Durrance (1980) extended the calculation of the dependence of transition moment on r using data of Lassettre and Skerbele (1971) and Mumma et al.(1971), and found a quadratic dependence on r. Durrance calculated oscillator strengths up to v'=14 and branching ratios up to v'=14 and v"=15. Durrance examined the credibility of his values using a least square fit , and concluded that his values are credible. We adopted his values for the v'= 10-12 states, which were used for the calculations of Einstein A coefficients for the v'= 10-12 → v"=13-15 transitions. We calculate an excitation rate of 4 x 10^{-7} sec^{-1} for the v"=0 → v'=1 transition, and present the value in Table 2.

An Einstein A coefficient for a rotational line is given by

$$A_{j'j"} = \frac{1}{1.499} \frac{\omega^3_{j'j"}}{\omega_{v'v"}} \frac{(2 - \Delta_{0,\lambda"}) f_{v'v"} H - L}{(2 - \Delta_{0,\lambda'+\lambda"})(2j' + 1)} \tag{4}$$

which is the same as Eq. (A7) of Schleicher and A'Hearn (1982). Here $\omega_{j'j"}$ is the wavenumber of a line, $f_{v'v"}$ is the oscillator strength, and H-L is the Hänl-London factor. Combining Eqs. (3) and (4), we obtain a relation between $A_{j'j"}$ and $A_{v'v"}$,as follow:

$$A_{j'j"} = \frac{(2 - \Delta_{0,\lambda'})}{(2 - \Delta_{0,\lambda'+\lambda"})} \frac{\omega^3_{j'j"}}{\omega^3_{v'v"}} A_{v'v"} \frac{H - L}{(2j' + 1)} \tag{5}$$

Eq. (5) becomes:

$$A_{j'j"} = \frac{\omega^3_{j'j"}}{\omega^3_{v'v"}} A_{v'v"} \frac{H - L}{(2j' + 1)} \tag{6}$$

It should be noted that the following normalization must be used for the H-L factors:

$$\Sigma_{p'p"} \Sigma_{\Sigma'\Sigma"} \Sigma_{j"} H - L = (2 - \Delta_{0,\lambda'+\lambda"})(2S' + 1)(2j' + 1) \tag{7}$$

Where S is the spin, Σ is the electronic substate due to spin multiplicity, and p is the parity. For the $A^1\Pi$ - $X^1\Sigma$ system, Eq. (7) yields 2 (2j' + 1). The H-L factors adopted from tables of Kovác (1969) have been normalized using Eq. (7), as follows:

H-L (P branch) = j'

H-L (Q branch) = 2j' + 1 (8)

H-L (R branch) = j' + 1

Einstein B coefficients were calculated from $A'_j j"$ using the following relation:

$$B_{j"j'} = \frac{1}{8\Pi h} \lambda^3_{j'j"} \frac{2j' + 1}{2j" + 1} A_{j'j"} \tag{9}$$

where h is the Planck constant. Eq. (9) is identical to Eq. (6) of Schleicher and A'Hearn (1982). The calculated $A_{j'j"}$ and $B_{j"j'}$ have been used to construct the fluorescence models of the A-X bands presented in the next section.

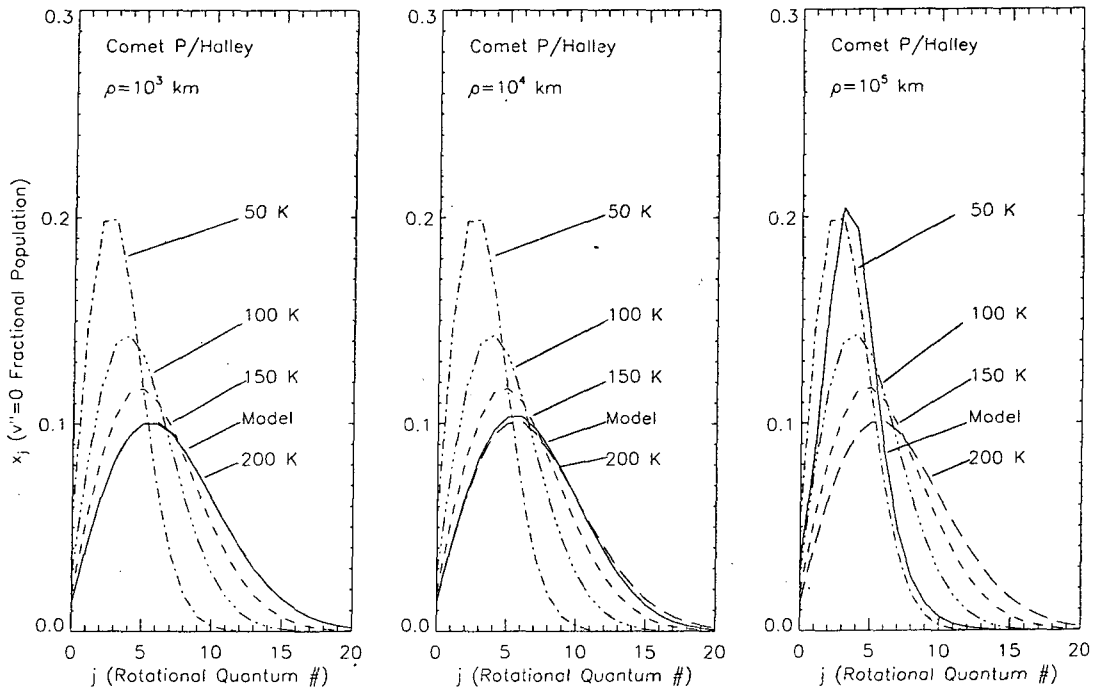

Fig. 1. Populations of CO for v"=0 as a function of rotational quantum number j at cometocentric distances (ρ) of 10^3, 10^4, and 10^5 km, respectively, for comet P/Halley. In these models we do not include infrared Swings effects in order to investigate neutral and electron collisional effects only. In these figures, we also present Boltzmann distributions at 50, 100, 150, and 200 K, for comparison. As seen in Figure 1a, at $\rho = 10^3$ km the distribution of v"=0 is indistinguishable from the 200 K Boltzmann distribution, but the distribution is deviated from the Boltzmann distribution significantly at $\rho = 10^4$ and 10^5 km.

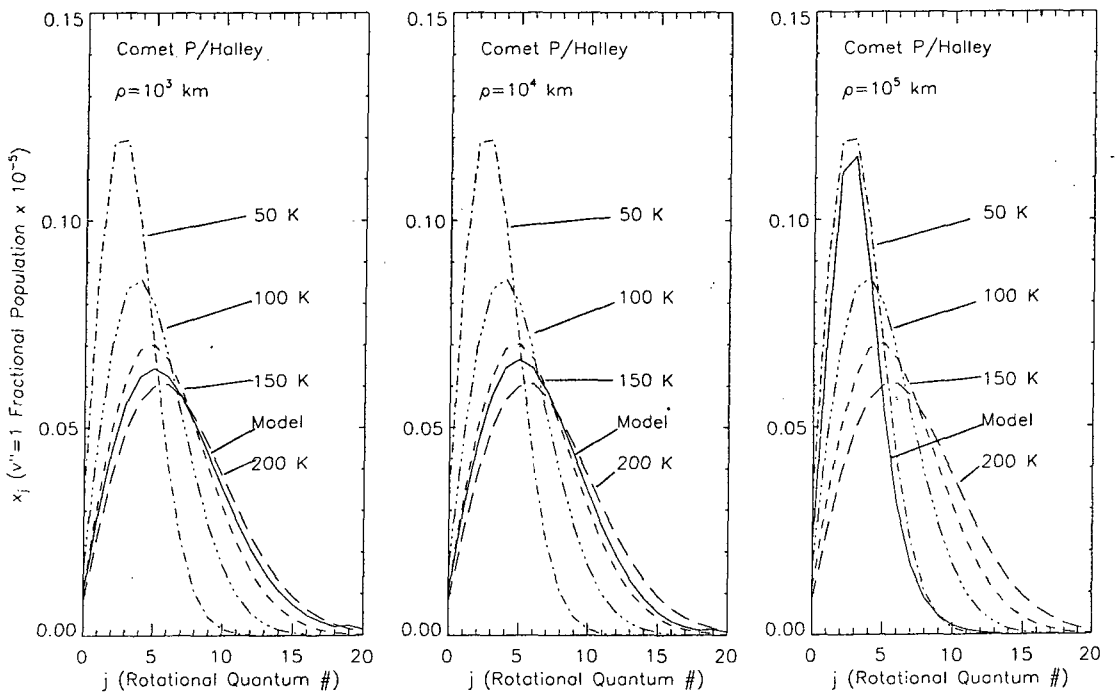

Fig. 2. The same populations as Figures 1a, 1b, and 1c, but for v"=1. The models do not include the infrared Swings effects. It is interesting to note that the shape of the v"=1 distribution is similar to the corresponding v"=0 distribution at the same cometocentric distance, although the absolute values of v"=1 are 5 orders of magnitude less than those of v"=0.

(d) Fluorescence Calculations

i) Infrared bands

As we discussed in the previous sections (and shown in Tabel 2), ro-vibrational transitions are dominant processes in determining the ground state population, whereas electronic transitions have negligible effects. Because the majority of CO molecules in the coma is in the ground rotational states (v"=0), we first calculate populations of ground ro-vibrational states as functions of heliocentric velocity and cometocentric distance. We include neutral and electron collisions, and excitations by solar radiation in the infrared band model. We consider v"= 0 and 1 including 30 rotational states for each vibrational state. In order to calculate a fractional population at each state, we assume statistical equilibrium and solve 60 simultaneous equations. Since the important infrared excitation or deexcitation times (which are inverse of the various transition rates presented in the previous section) are substantially shorter than the CO lifetime, which is about 10^6 sec at 1 AU, the equilibrium assumption is reasonable.

Figures 1a, 1b, and 1c present results of the fluorescence calculations for the populations of v"=0 as a function of rotational quantum number j at cometocentric distances (ρ) of 10^3, 10^4, and 10^5 km, respectively, for comet P/Halley. In these models we do *not* include infrared Swings effects in order to investigate neutral and electron collisional effects only. In these figures, we also present Boltzmann distributions at 50, 100, 150, and 200 K, for comparison. As seen in Figure 1a, at $\rho = 10^3$ km the distribution of v"=0 is indistinguishable from the 200 K Boltzmann distribution, but the distribution is deviated from the Boltzmann distribution noticeably at $\rho = 10^4$ km. At $\rho = 10^5$ km and $\rho = 10^6$ km (which is not shown here), the rotational distribution is close to 50 K significantly different from surrounding temperature, which is approximately 200 K (Crifo, 1992). Figures 2a, 2b, and 2c present the same populations for v"=1 at $\rho = 10^3$, 10^4, and 10^5 km, respectively. The models do not include the infrared Swings effects. It is interesting to note that the shape of the v"=1 distribution is almost identical to the corresponding v"=0 distribution at the same cometocentric distance, although the absolute values of v"=1 are 5 orders of magnitude less than those of v"=0.

Infrared solar spectrum contains strong absorption lines of the fundamental band and hot bands of solar CO and its isotopes. According to the high resolution solar infrared spectrum obtained by the ATMOS investigation on the Spacelab 3 Mission, absorption depths of strong CO lines are about 20 - 25 adjacent continuum in the 5 micron region, where the fundamental band of CO occurs. Other than the CO lines, the 5 micron solar continuum is fairly flat. The full-width-half-maximum of the solar CO lines is about 0.05 cm^{-1}, which corresponds to about 7.5 km/sec around 5 microns. We expect significant Swings effects within heliocentric velocities of $\pm$ 5.0 km/sec. Since the comet Halley UV spectra were taken at heliocentric velocities greater than 5 km/sec, the Swings effect on individual lines of the UV band caused by infrared solar pumping is negligible. However, recent HST spectra of comet Shoemaker-Levy (1991a1) were taken near 0 km/sec heliocentric velocities, and the infrared Swings effect on individual lines of a UV band may be noticeable, although the overall infrared Swings effect on a UV band is negligible as we will discuss in the later section.

In Figures 3a and 3b we present v" = 0 and v" = 1 distributions as a function of j, respectively, at $\rho = 10^3$ km for r = -20, -10, 0, 10, 20 km/sec. In Figures 3c and 3d we present the same distributions at $\rho = 10^5$ km. In these models, Swings effects have been included. As shown in Figure 3a, however, we do not see any Swings effects on the v" =0 distribution. This is because at ρ is equal or less than 10^3 km, excitations by neutral collisions are totally dominant over the solar infrared excitation rendering the distribution a Boltzmann distribution for all of those velocities. In Figure 3b, however, we see v"=1 distributions significantly deviated from Boltzmann distribution. In particular, at r = 0 km/sec, the overall population is 20 at other velocities. This indicates low solar excitation at the centers of CO lines. Figure 3c shows v"=0 distributions at $\rho = 10^5$ km. The distributions are significantly deviated from Boltzmann distribution because at $\rho = 10^5$ km neutral collisions are not dominant excitation mechanisms and electron collisions and solar infrared pumping rates become dominant excitations. We however note that summations of the distributions over j at v"=0 are about 0.99999 for all the heliocentric velocities at $\rho = 10^3$ and 10^5 km. The difference of the summed population between 0 and 20 km/sec is only 0.000002 at $\rho = 10^3$ and10^5 km. It is interesting that individual j state population varies up to 0.015 in terms of fractional population for different heliocentric velocities, yet the summed population over j varies only up to 0.000002 for different heliocentric velocities. This is because all the over populated j states (compared with Boltzmann distribution) due to less active solar pumping are formed at the expense of under populated j states due to active solar pumping, and therefore the summed population is

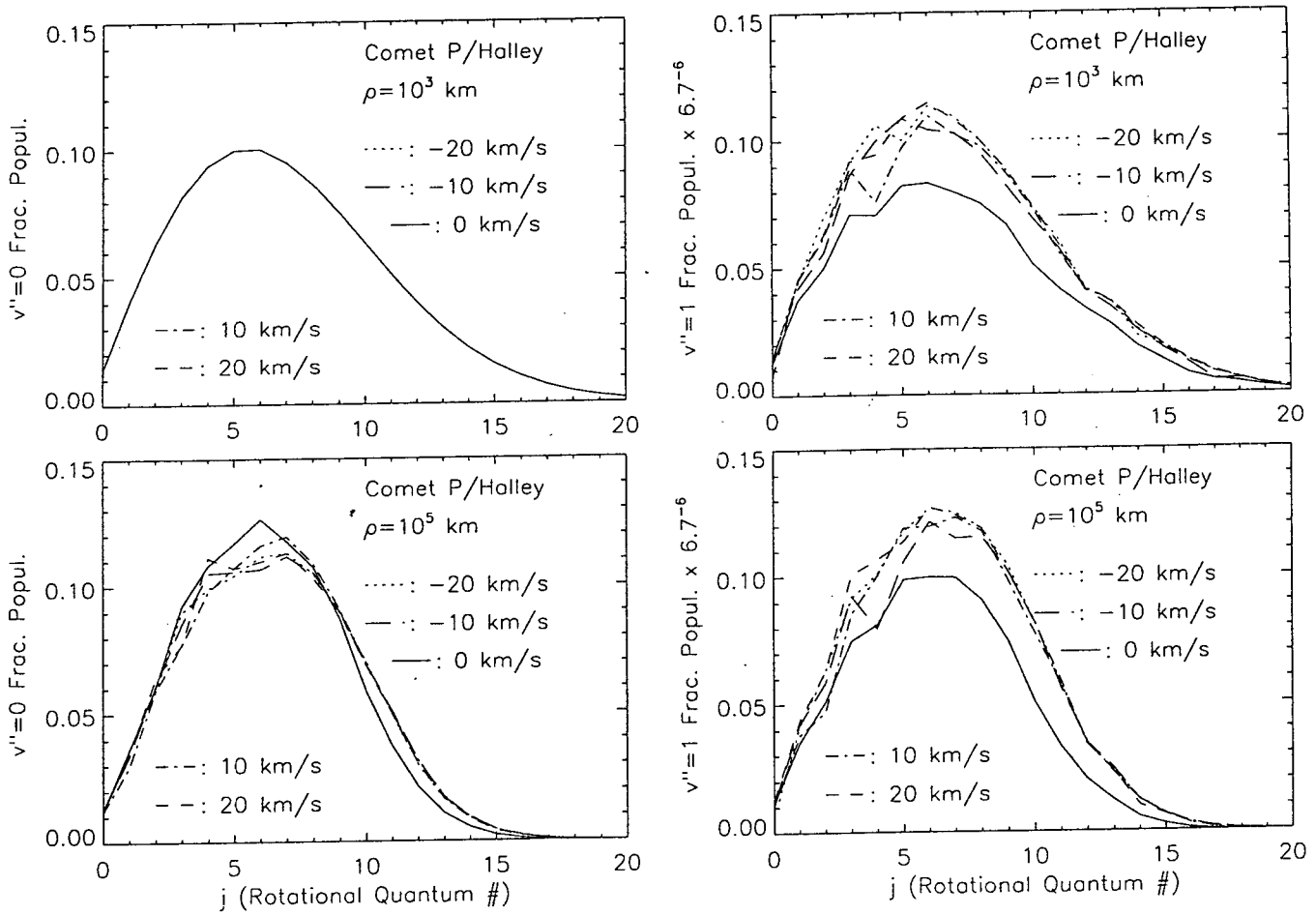

Fig. 3. Show v"=0 and v"=1 distributions as a function of j, respectively, at $\rho = 10^3$ km for r = -20, -10, 0, 10, 20 km/sec. In Figures 3c and 3d, we present the same distributions at $\rho = 10^5$ km. In these models, Swings effects have been included. As shown in Figure 3a, however, we do not see any Swings effects on the v"=0 distribution. This is because at ρ is equal or less than 10^3 km, excitations by neutral collisions are totally dominant over the solar infrared excitation rendering the distribution a Boltzmann distribution for all of those velocities. In Figure 3b, however, we see v"=1 distributions significantly deviated from Boltzmann distribution. In particular, at r = 0 km/sec, the overall population is 20 other velocities. This indicates low solar excitation at the centers of CO lines. Figures 3c and 3d show distributions significantly deviated from Boltzmann distribution because at $\rho = 10^5$ km neutral collisions are not dominant excitation mechanisms and electron collisions and solar infrared pumping rates become dominant excitations.

very close to 1.0. Figure 3d shows v"=1 distributions at $\rho = 10^5$ km. At v"= 1 summed population over j at r = 0 km/sec is clearly less (about 20other heliocentric velocities because of less solar pumping around the centers of solar CO lines. Figures 4a and 4b show intensity distributions (g-factors) of the rotational lines of the v"=1 → 0 band at r = 0 and -20 km/sec, respectively, at $\rho = 10^3$ km. Figures 4c and 4d show the same distributions at $\rho = 10^5$ km. These figures demonstrate that not only the total band intensities but individual relative line intensities are significantly different depending upon heliocentric velocity or cometocentric distance.

There are two major differences between the model of Chin and Weaver (1984) and our model: (1) Chin and Weaver did not include infrared Swings effects; and (2) Chin and Weaver assumed that CO is only produced from nucleus, and they conducted non-equilibrium fluorescence calculation as CO undergoes various fluorescence and collisional processes from cometary surface through inner coma to outer coma. Since Eberhardt et al. (1987) found in comet P/Halley there should be an extended source producing CO up to the same amount from the nucleus, we chose fluorescent equilibrium calculations because the CO lifetime is longer than the most transition rates. We found that g-factors of the individual lines of the band differ mostly within a factor of two for low j lines, and sometimes

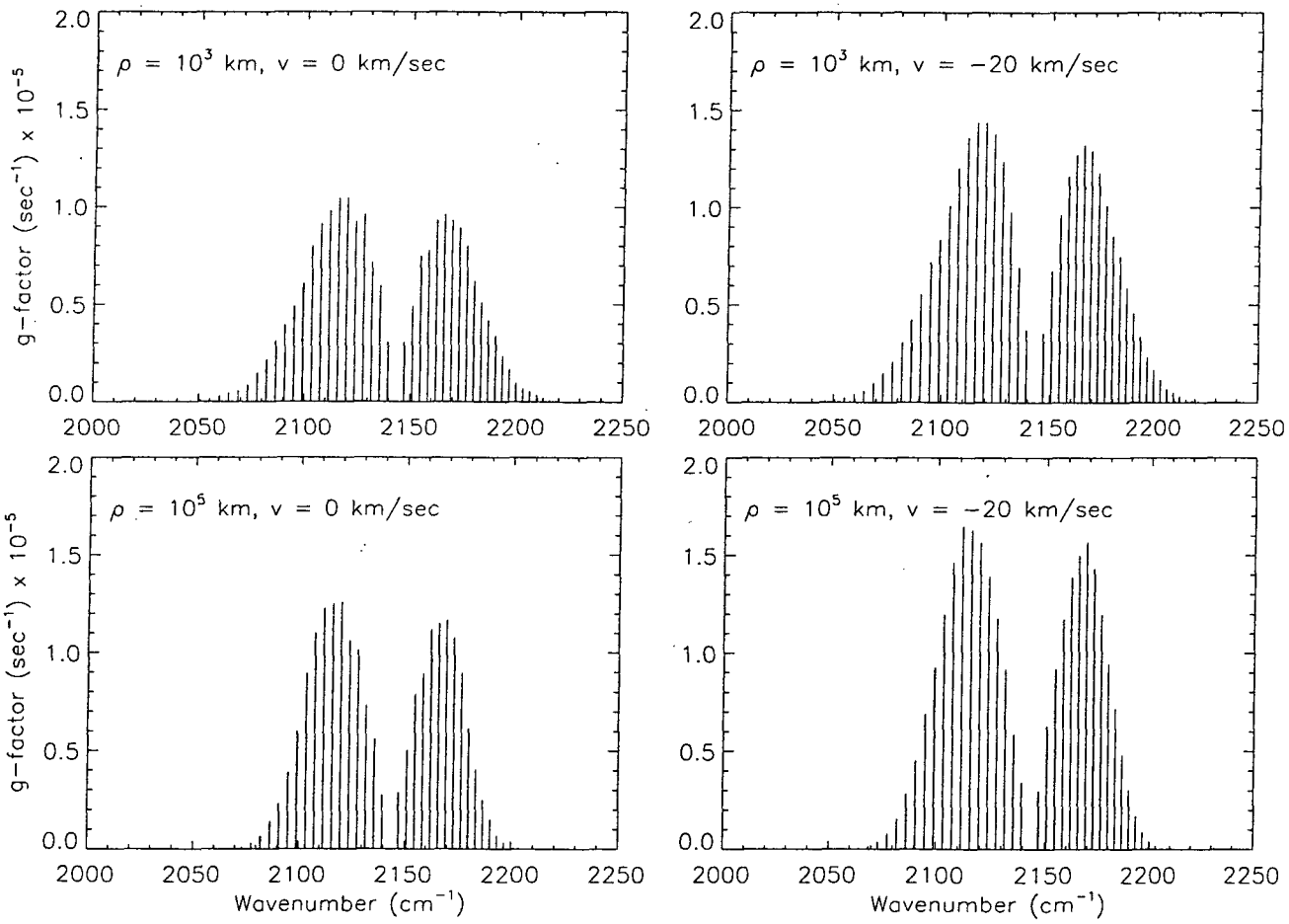

Fig. 4. Show intensity distributions (g-factors) of the rotational lines of the v"=1 → 0 band at r = 0 and -20 km/sec, respectively, at $\rho = 10^3$ km. Figures 4c and 4d show the same distributions at $\rho = 10^5$ km. These results demonstrate that not only the total band intensities but individual relative line intensities are different depending upon heliocentric velocity or cometocentric distance.

more than a factor of two for high j lines between two models (Chin and Weaver's vs ours) throughout various different conditions and different cometocentric distances.

Figures 5a and 5b show total g-factors of the v"=1 → 0 band for $\rho = 10^3$ and 10^6 km, respectively, as a function of heliocentric velocity between -75 and +75 km/sec. As seen in the two figures, the shapes of g-factors are remarkably the same between two cometocentric distances. We note that the solar CO absorption lines cause a 20 fundamental band at r 0 km/sec.

ii) Ultraviolet bands

Solar radiation in the 1200 - 2000 $\dot{A}$ range shows significant temporal variation during a day, month, year, and 11 year solar cycle time scale (e.g. Lean, 1991). For example, the solar continuum around 1500 $\dot{A}$ can vary up to almost 200 intensities of sharp emission lines are expected to vary more. In general shorter wavelength region (¡ 2000 $\dot{A}$) shows high temporal variation compared with longer wavelength region (¿ 2000 $\dot{A}$), and around 3000 $\dot{A}$ the temporal variation is less than 1 solar cycle. One must take account of solar variability in order to properly calculate accurate g-factors of the CO A-X system. It would also be ideal to have a high resolution full-disk solar spectrum taken at the time of comet observations. Available high resolution solar spectra are however scarce, although the Orbiting Solar Observatory (OSO) 8 had been in operation between 1975 and 1978, and next the Solar Maximum Mission (SMM) had been in operation between 1980 and 1989 with a high resolution spectrometer. To our knowledge there is no available full-disk high resolution spectrum (private communications with J. Gurman, 1992).

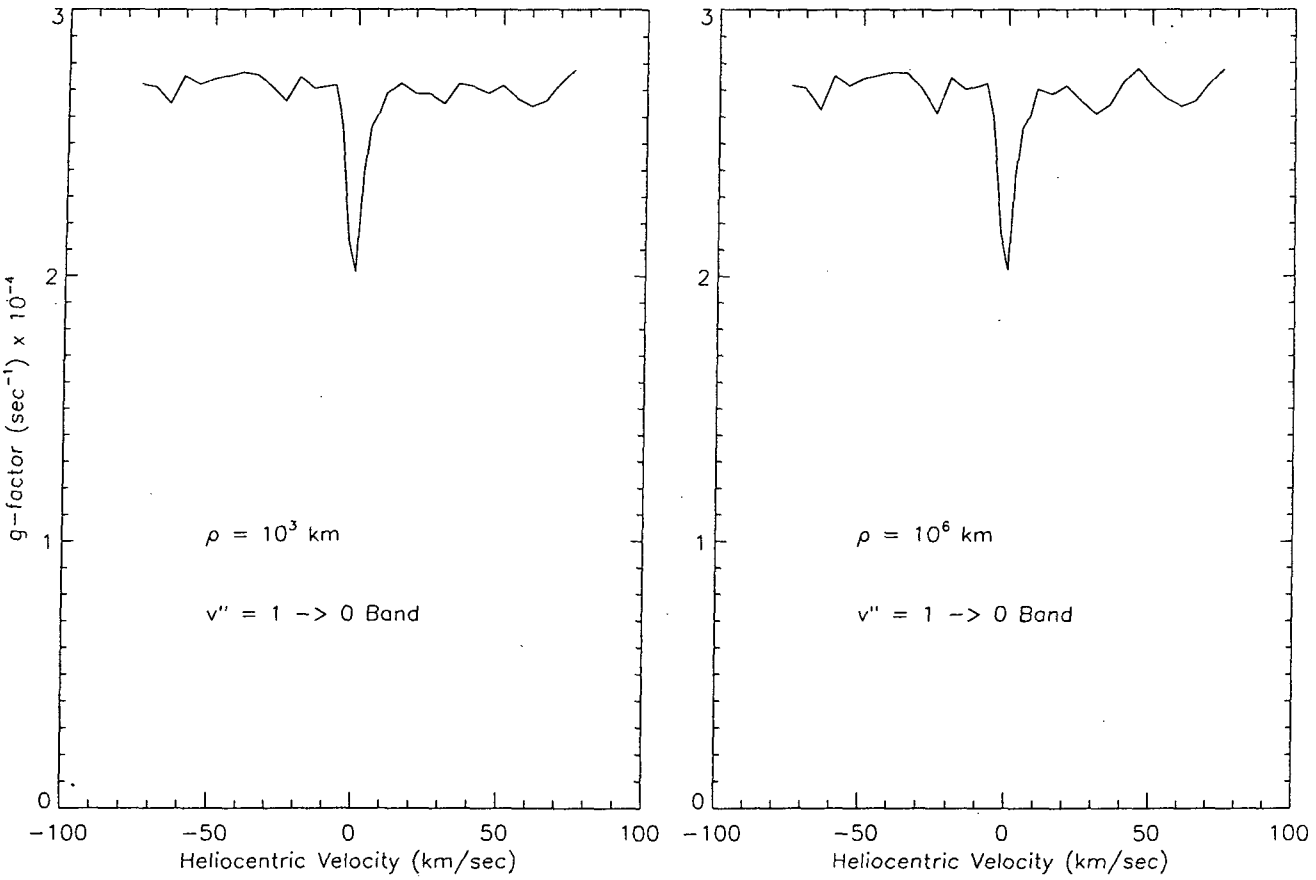

Fig. 5. Show total g-factors of the v"=1 → 0 band for ρ =10^3 and 10^6 km, respectively, as a function of heliocentric velocity between -75 and +75 km/sec. As seen in these figures, the shapes of g-factors are remarkably the same between two cometocentric distance. We note that the solar CO absorption lines cause a 20 fundamental band at r 0 km/sec.

Recently Brekke (1993) presented high resolution solar spectra of active region, quiet region, sun spot, lightbridge in sun spot, etc. The data were obtained with the High Resolution Telescope and Spectrograph (HRTS) during a rocket flight in 1978. The spectral resolution of the instrument was 0.05 $\dot{A}$ while a spatial resolution of approximately 1.8" was achieved. These solar spectra covering the 1190 - 1730 $\dot{A}$ range were provided to us by Dr. P. Brekke (private communications, 1993). We were also able to obtain a high resolution ($\Delta\lambda$ = 0.03$\dot{A}$) spectrum in the 1290 - 1770 $\dot{A}$ range of the sun from the SMM data center. The entrance aperture size was a 1" × 180", with the long direction running north to south on the sun. This spectrum is a mosaic of more than 10 spectra taken at different times in 1980 and 1984 when the solar activities were in maximum and relatively quiet, respectively. This mosaic was done because the spectrometer on the SMM usually took a limited spectral range (usually a 10 - 20 $\dot{A}$ wavelength step) during an orbit. It of course does not represent the full-disk solar spectrum. J. Lean provided a full-disk solar spectrum with a 0.5 $\dot{A}$ resolution in the 1200 - 4030 $\dot{A}$ region taken on August 3, 1985. Since the Lean's full-disk spectrum was obtained during the quiet sun period, the spectrum has been used for a rough analysis of low-resolution IUE Halley spectra and for obtaining approximate g-factors of the A-X bands during the quiet solar activity, as discussed below. We present a discussion in Appendix A on the possible derivation of a synthesized full-disk solar spectrum at a given time using high resolution spectra of active and quiet regions.

In order to derive UV Swings effects of the CO bands, we used the SMM spectrum (we could use Brekke's spectra, but they are not full-disk spectra either). For the 1770 - 2100 $\dot{A}$ range, we adopted a high resolution spectrum from a rocket observation (Kjeldseth Moe, et al. 1976). For the 1200 - 1290 $\dot{A}$ and 2100 - 2400 $\dot{A}$ ranges, we adopted

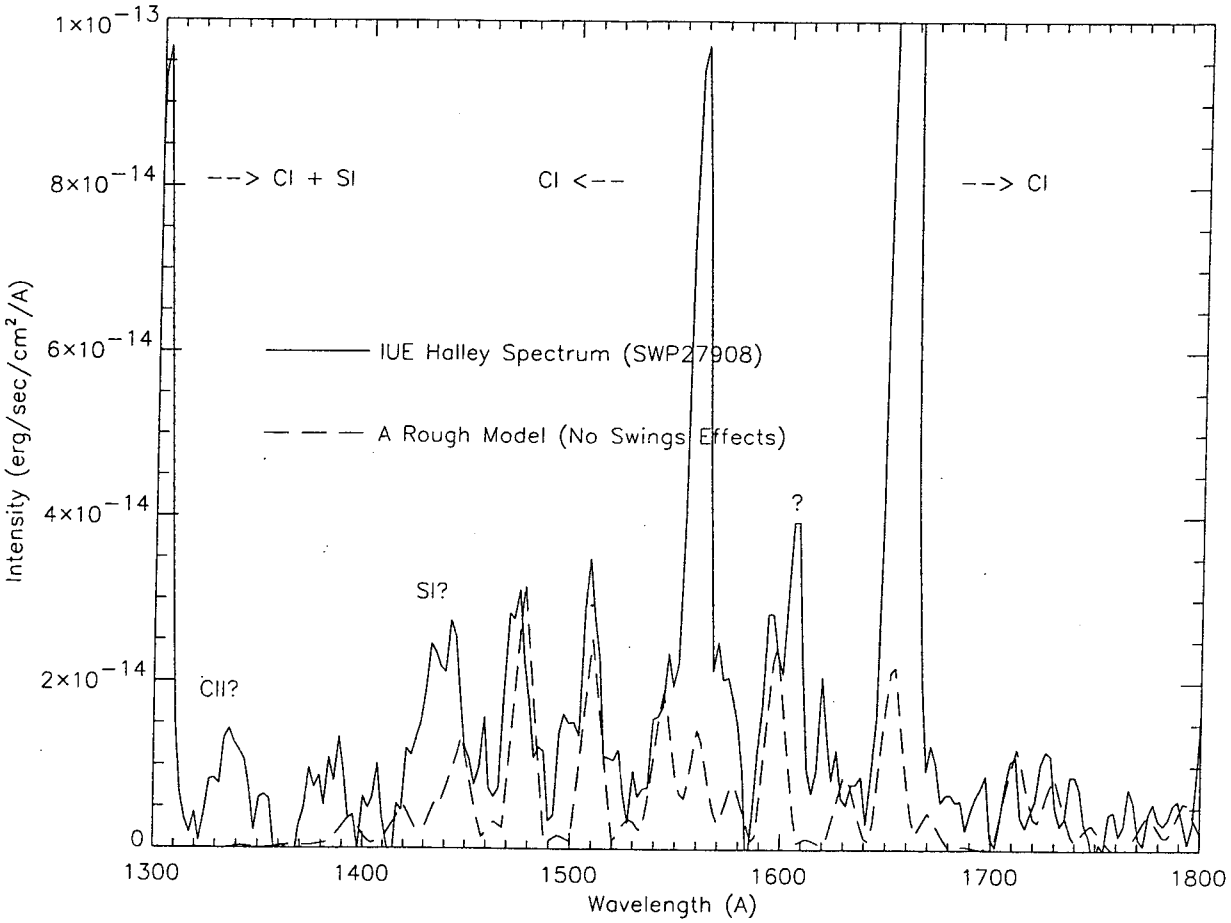

Fig. 6. A comparison between a rough fluorescence equilibrium model, which includes only vibrational transitions of the A-X system (excluding all rotational transitions), and the Halley spectrum. The model does not include the Swings effects, and vibrational band heads were convolved with a triangular function with a FWHM of 10 $\dot{A}$. The calculated fractional populations for the vibrational states in the A and X states at 1 AU are summarized in Table 3. We also present g-factors of the CO bands from this rough model in Table 4.

the medium resolution spectrum ($\Delta\lambda = 0.5\dot{A}$) provided by J. Lean . Above 2400 A we adopted a high resolution full-disk spectrum compiled by A'Hearn, et al. (1983). We expect that adopting the Lean's spectrum in the 1200 - 1290 $\dot{A}$ and 2100 - 2400 $\dot{A}$ ranges do not cause significant effects on the model because CO lines are very weak in the ranges. We found that between 1300 and 1400 $\dot{A}$ the continuum and line intensities of the SMM spectrum are at least a factor of two greater than those of the Lean's full disk spectrum. Between 1500 and 1800 $\dot{A}$ the difference between two spectra is less than 15 we discussed later, the UV Swings effect on the g-factors is less than 20 solar continuum and the oscillator strength uncertainty can cause 100 therefore used the high resolution SMM spectrum only to see *relative* g-factor variation as a function of heliocentric velocity, although absolute values of the g-factors are not reliable. The Lean's full-disk solar spectrum was used for the derivation of the *absolute* values of g-factors of the CO bands including only vibrational transitions, which will be discussed in the second next paragraph.

As we discussed before, the pure vibrational-rotational transitions determine the ground rotational-state populations, which are almost independent from UV transitions. Chin and Weaver ignored the UV transitions and other vibrational transitions except v" =0 and 1. This approach used by Chin and Weaver (1984) is a good approximationbecause the transitions between v" =0 and 1 are totally dominant fluorescence processes over other vibrational and electronic transitions The most significant uncertainty in their model rather comes from the following two simplifications : (1) they assumed all the CO coming from the nucleus; and (2) they ignored any infrared Swings effects. For a reasonable approximation, therefore, we have used the v" =0 and 1 populations derived from the infrared

band model calculations and a single cycle UV fluorescence to calculate g-factors of the UV bands. The uncertainty arising from this approximation is significantly less than other uncertainties arising from temporal variation of solar radiation plus uncertainty in oscillatorstrengths mentioned above. Durrance (1980) basically used only v" =0 state in the X state and a single fluorescence calculation to obtain the g-factors of the UV bands, although he did not include UV Swings effects and used a Boltzmann distribution for the rotational population for v" =0 state.

Table 3. The calculated fractional populations, x_v, for the vibrational states in the A and X states at 1 AU for a quiet sun.

X state		A state	
v"	$x_{v"}$	v'	$x_{v'}$
0	0.100E+01	0	0.498E-14
1	0.676E-05	1	0.381E-14
2	0.351E-05	2	0.410E-14
3	0.244E-05	3	0.194E-14
4	0.190E-05	4	0.971E-15
5	0.158E-05	5	0.112E-14
6	0.138E-05	6	0.187E-15
7	0.122E-05	7	0.804E-16
8	0.111E-05	8	0.347E-16
9	0.103E-05	9	0.855E-16
10	0.961E-06	10	0.237E-16
11	0.906E-06	11	0.341E-16
12	0.866E-06	12	0.301E-16
13	0.835E-06		
14	0.799E-06		
15	0.771E-06		
16	0.751E-06		
17	0.730E-06		
18	0.714E-06		
19	0.699E-06		
20	0.683E-06		
21	0.672E-06		
22	0.659E-06		
23	0.650E-06		
24	0.644E-06		

We first performed a fluorescence calculation without considering Swings effects. For the fractional populations of the states v" ¿ 1, we used a rough fluorescence equilibrium model, which includes only vibrational transitions of the A-X system (excluding all rotational transitions), and using a smoothed solar spectrum. The smoothed spectrum was obtained by binning the Lean's spectrum with a 10 A interval, which is about the same as the spectral resolution of the IUE Halley spectra. The reasons that this approximation is reasonable are: (1) the inclusion of the v" ¿ 1 states do not influence overall UV g-factor calculations significantly because of low populations in these states; and (2) since the CO lines in the UV bands are highly accumulated, the Swings effects on individual lines tends to be canceled out. We present this rough model in Figure 6 compared with a Halley spectrum. The model of couse does not include the Swings effects, and monochromatic vibrational band heads were convolved with a triangular function with a FWHM of 10 $\AA$. The fit is reasonable considering the noise level in the IUE spectrum. The calculated fractional populations for the vibrational states in the A and X states at 1 AU for a quiet sun (i.e., using the Lean's spectrum) are summarized in Table 3. We also present g-factors of the CO bands from this rough model in Table 4.

Table 4. g-factors of the bands of the CO A-X system for a quiet sun at 1 AU. The model does not include Swings effects, and it is a rough model including vibrational transitions and ignoring rotational transitions. See the main text for the accuracy of this model.

v'	v"	$\lambda(\dot{A})$	$g(sec^{-1})$	v'	v"	$\lambda(\dot{A})$	$g(sec^{-1})$
0	0	1544.4	9.313E-08	0	1	1597.3	1.698E-07
1	0	1509.9	1.604E-07	1	1	1560.4	8.915E-08
2	0	1477.8	2.116E-07	2	1	1526.1	7.052E-09
3	0	1447.8	8.866E-08	3	1	1494.2	1.034E-08
4	0	1419.8	3.250E-08	4	1	1464.3	2.239E-08
5	0	1393.6	2.496E-08	5	1	1436.5	4.152E-08
6	0	1369.1	2.478E-09	6	1	1410.4	7.350E-09
7	0	1346.1	5.365E-10	7	1	1386.1	2.417E-09
8	0	1324.5	1.130E-10	8	1	1363.2	7.092E-10
9	0	1304.3	1.371E-10	9	1	1341.9	1.118E-09
10	0	1285.4	1.741E-11	10	1	1321.8	1.750E-10
11	0	1267.6	1.145E-11	11	1	1303.0	1.389E-10
12	0	1250.9	4.586E-12	12	1	1285.4	6.552E-11
0	2	1653.2	1.454E-07	0	3	1712.4	7.769E-08
1	2	1613.7	1.105E-09	1	3	1670.1	2.896E-08
2	2	1577.1	5.535E-08	2	3	1630.8	5.207E-08
3	2	1543.0	3.667E-08	3	3	1594.4	8.808E-12
4	2	1511.2	5.126E-09	4	3	1560.5	9.820E-09
5	2	1481.5	5.880E-10	5	3	1528.9	1.896E-08
6	2	1453.8	2.247E-09	6	3	1499.4	1.388E-09
7	2	1428.0	2.031E-09	7	3	1471.9	1.903E-12
8	2	1403.8	1.087E-09	8	3	1446.2	1.778E-10
9	2	1381.1	2.616E-09	9	3	1422.1	1.416E-09
10	2	1359.9	5.612E-10	10	3	1399.6	5.827E-10
11	2	1340.0	5.782E-10	11	3	1378.6	9.116E-10
12	2	1321.3	3.377E-10	12	3	1358.9	7.333E-10
0	4	1775.1	2.893E-08	0	5	1841.7	7.918E-09
1	4	1729.7	5.486E-08	1	5	1792.8	3.962E-08
2	4	1687.6	1.185E-09	2	5	1747.7	1.788E-08
3	4	1648.6	1.932E-08	3	5	1705.9	1.238E-08
4	4	1612.4	7.090E-09	4	5	1667.1	1.021E-09
5	4	1578.7	1.200E-10	5	5	1631.1	1.163E-08
6	4	1547.3	1.806E-09	6	5	1597.6	8.988E-10
7	4	1518.0	1.166E-09	7	5	1566.4	2.622E-11
8	4	1490.7	2.603E-10	8	5	1537.3	2.696E-10
9	4	1465.1	4.681E-11	9	5	1510.2	1.082E-09
10	4	1441.3	5.375E-11	10	5	1484.9	1.675E-10
11	4	1418.9	3.481E-10	11	5	1461.2	3.717E-11
12	4	1398.1	5.494E-10	12	5	1439.0	1.812E-11

Table 4. (continued)

v'	v"	$\lambda(\dot{A})$	$g(sec^{-1})$	v'	v"	$\lambda(\dot{A})$	$g(sec^{-1})$
0	6	1912.5	1.658E-09	0	7	1987.9	2.709E-10
1	6	1859.9	1.692E-08	1	7	1931.1	4.953E-09
2	6	1811.3	3.624E-08	2	7	1878.9	2.616E-08
3	6	1766.5	3.515E-11	3	7	1830.6	7.217E-09
4	6	1725.0	7.542E-09	4	7	1786.1	2.455E-09
5	6	1686.4	1.620E-09	5	7	1744.8	3.456E-09
6	6	1650.6	6.846E-10	6	7	1706.5	1.155E-09
7	6	1617.4	7.190E-10	7	7	1671.0	1.765E-12
8	6	1586.4	9.684E-11	8	7	1637.9	1.656E-10
9	6	1557.5	3.761E-11	9	7	1607.1	6.323E-10
10	6	1530.5	1.557E-10	10	7	1578.5	3.763E-11
11	6	1505.4	3.481E-10	11	7	1551.7	1.690E-11
12	6	1481.9	2.180E-10	12	7	1526.8	1.570E-10
0	8	2068.4	3.521E-11	0	9	2154.4	3.685E-12
1	8	2007.0	1.059E-09	1	9	2087.9	1.730E-10
2	8	1950.6	1.095E-08	2	9	2026.9	3.108E-09
3	8	1898.7	1.129E-08	3	9	1970.9	7.236E-09
4	8	1850.8	2.809E-10	4	9	1919.3	3.221E-09
5	8	1806.5	5.904E-09	5	9	1871.8	6.540E-10
6	8	1765.5	2.018E-12	6	9	1827.8	7.560E-10
7	8	1727.5	4.276E-10	7	9	1787.1	1.345E-10
8	8	1692.2	1.015E-10	8	9	1749.3	4.752E-11
9	8	1659.3	2.300E-11	9	9	1714.3	4.339E-10
10	8	1628.8	1.198E-10	10	9	1681.7	2.365E-11
11	8	1600.3	1.864E-10	11	9	1651.4	2.915E-11
12	8	1573.8	3.906E-11	12	9	1623.2	1.421E-10
0	10	2246.6	2.988E-13	0	11	2345.5	1.833E-13
1	10	2174.3	2.202E-11	1	11	2266.9	1.577E-11
2	10	2108.3	6.396E-10	2	11	2195.2	9.881E-11
3	10	2047.8	2.755E-09	3	11	2129.6	7.217E-10
4	10	1992.2	3.663E-09	4	11	2069.6	1.984E-09
5	10	1940.9	9.732E-10	5	11	2014.4	3.156E-09
6	10	1893.7	4.956E-10	6	11	1963.5	1.054E-12
7	10	1850.0	7.310E-11	7	11	1916.6	2.460E-10
8	10	1809.6	1.253E-10	8	11	1873.2	1.876E-12
9	10	1772.1	5.809E-12	9	11	1833.1	2.372E-10
10	10	1737.3	6.536E-11	10	11	1795.9	3.741E-11
11	10	1705.0	1.198E-10	11	11	1761.4	8.791E-12
12	10	1674.9	1.081E-11	12	11	1729.3	9.349E-11

Next we performed a line-by-line fluorescence calculation including Swings effects. The total number of states involved in the UV fluorescence equilibrium calculations are about 840. Therefore, it is not practical to solve 840 simultaneous equations, although it is not impossible. If we have a reasonable scientific justification, it is desirable

Table 4. (continued)

v'	v"	$\lambda(\dot{A})$	g(sec^{-1})	v'	v"	$\lambda(\dot{A})$	g(sec^{-1})
0	12	2452.0	1.549E-14	12 0	13	2566.8	1.111E-15
1	12	2366.1	1.871E-12	12 1	13	2472.9	1.852E-13
2	12	2288.1	1.168E-11	12 2	13	2387.8	1.931E-12
3	12	2217.0	1.362E-10	12 3	13	2310.5	2.755E-11
4	12	2152.0	6.678E-10	12 4	13	2239.9	2.023E-10
5	12	2092.4	2.652E-09	12 5	13	2175.4	1.452E-09
6	12	2037.6	2.352E-10	12 6	13	2116.2	4.515E-10
7	12	1987.1	6.196E-11	12 7	13	2061.8	1.560E-11
8	12	1940.5	5.796E-11	12 8	13	2011.7	6.192E-11
9	12	1897.5	1.109E-10	12 9	13	1965.5	2.823E-11
10	12	1857.6	1.559E-11	12 10	13	1922.8	4.859E-11
11	12	1820.7	9.086E-11	12 11	13	1883.3	1.587E-12
12	12	1786.5	1.416E-11	12 12	13	1846.7	4.712E-11
0	14	2690.9	6.723E-17	0	15	2825.6	3.421E-18
1	14	2587.9	1.535E-14	1	15	2712.2	1.067E-15
2	14	2494.9	1.771E-13	2	15	2610.2	1.345E-14
3	14	2410.6	3.608E-12	3	15	2518.1	3.861E-13
4	14	2333.9	3.997E-11	4	15	2434.5	6.196E-12
5	14	2263.9	4.764E-10	5	15	2358.5	1.142E-10
6	14	2199.9	3.150E-10	6	15	2289.1	1.338E-10
7	14	2141.2	1.166E-10	7	15	2225.6	1.311E-10
8	14	2087.2	2.833E-12	8	15	2167.3	1.732E-11
9	14	2037.5	1.588E-10	9	15	2113.8	6.170E-11
10	14	1991.6	2.146E-12	10	15	2064.5	1.877E-11
11	14	1949.3	4.809E-11	11	15	2019.0	2.797E-11
12	14	1910.1	2.974E-11	12	15	1977.0	8.392E-12

to use an approximation because the temporal variation of solar radiation and uncertainty in the oscillator strengths give siginificant uncertainty in the g-factors of the UV bands anyway. For the rotational distributions for v" ¿ 1, we adopted the v"=1 distribution adjusting only the total fractional populations given in Table 3. Once we determine the rotational and vibrational populations in the X state, we perform single fluorescence calculations to determine fractional populations in rotational and vibrational states of the A state. This is a good approximation because UV transitions negligibly affect the ground state populations, and only ro-vibrational transitions affect the ground state populations significantly. Excitation rates by solar UV radiation are obtained by multiplying $B_{v"j"v'j'}$ (Eq. 9) with monochromatic solar radiation densities $\rho_{v"j"v'j'}$, which is derived from the high resolution solar spectrum discussed before. The fractional populations at v'j' states in the A state are then given by:

$$x_{v'j'} = \frac{\Sigma_{v"j"} B_{v"j"v'j'} \rho_{v"j"v'j'} x_{v"j"}}{\Sigma_{v"j"} A_{v'j'v"j"}} \tag{10}$$

where the summation is strictly restricted by selection rules, and $x_{v"j"}$ is the fractional population in the X state. A g-factor for an individual line is then given by:

$$g_{v'j'v"j"} = x_{v'j'} A_{v'j'v"j"} \tag{11}$$

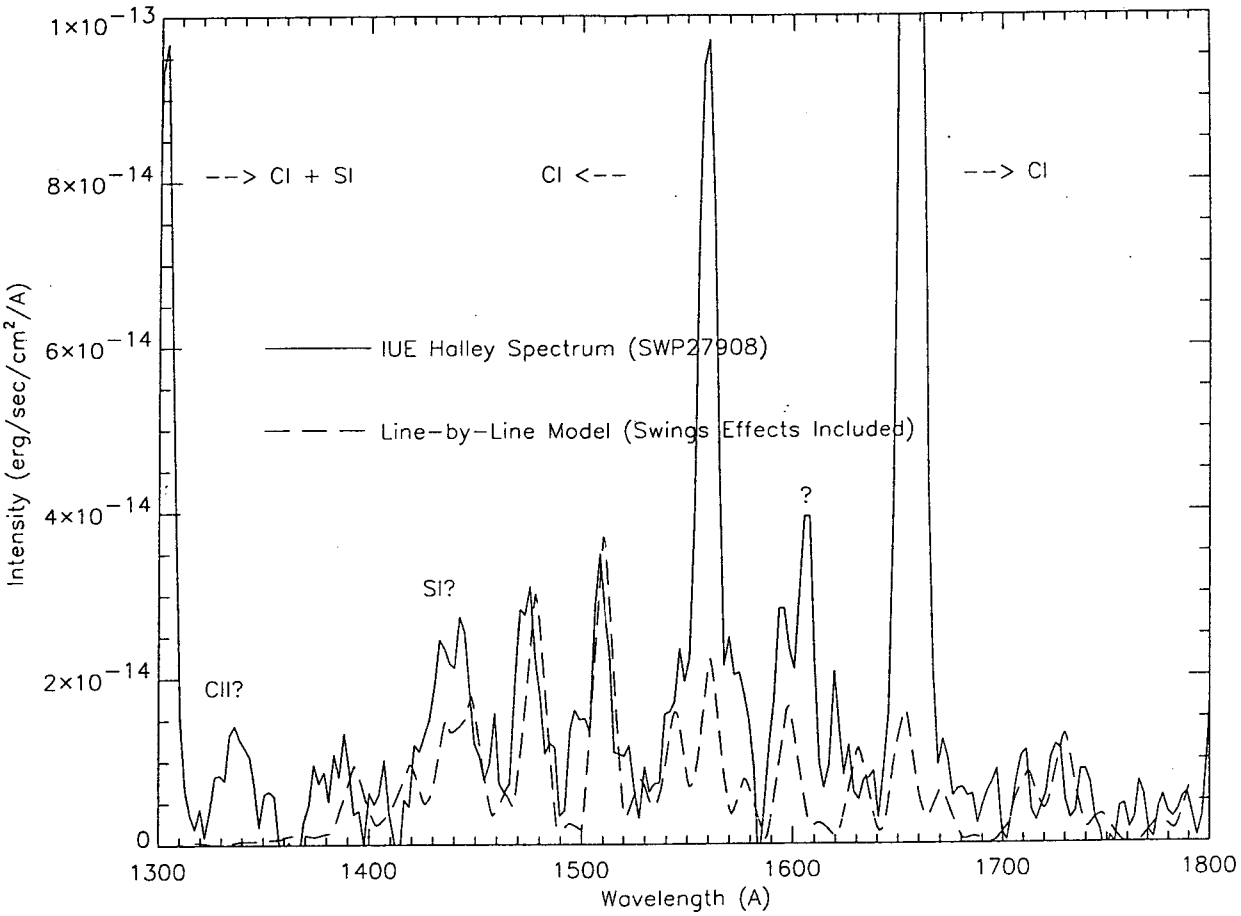

Fig. 7. A comparison between a line-by-line model of the A-X system and the Halley spectrum. The model includes the Swings effects, and monochromatic lines were convolved with a triangular function with a FWHM of 10 $\dot{A}$. This line-by-line model spectrum does not show dramatic difference from the rough model presented in Figure 6.

Figure 7 shows a line-by-line model compared with an IUE Halley spectrum. The model spectrum includes the Swings effect and collisional effects by neutrals and electrons. The model spectrum is a sum of properly weighted model spectra at various cometocentric distances within the IUE aperture and aperture rows where individual IUE spectra were taken. The model spectrum does not show dramatic difference from the rough model presented in Figure 6. During the model and observation comparison, we found excessive emissions in the 1200 - 1300 $\dot{A}$ and 1550 - 1630 $\dot{A}$ ranges. The excessive emissions were obtained after the elimination of the A-X band emission of CO using the CO band model, and other atomic emission lines. We note that the emission peaks of the B-X and C-X bands of H_2 occur in the 1100 - 1300 $\dot{A}$ and 1550 - 1630 $\dot{A}$ ranges. However, the excessive emissions in the 1200 - 1300 $\dot{A}$ region may be due to scattered light of Lyman-α, and the structure of the 1550 - 1630 $\dot{A}$ feature does not match well with the B-X band shape of H_2. The excessive emissions are not obvious in other IUE Halley spectra and HST spectra of Shoemaker-Levy (1991a1).

In Figure 8a, we present g-factors of 6 bands near 1443, 1480, 1510, 1600, 1710, and 1730 $\dot{A}$ at $\rho = 10^3$ km as a function of heliocentric velocity. As seen in this figure, the g-factors of the bands vary less than 20heliocentric velocities. In Figure 8b, we present the g-factors of the same 6 bands at $\rho = 10^6$ km. The difference in the g-factors betwen $\rho = 10^3$ and 10^6 km is usually less than 5 we caution readers again that the g-factors in Figs. 8a and b have been der ived from a line-by-line model using a high resolution solar spectrum, and the g-factors in Table 4 were derived from a rough model using a full-disk quiet sun spectrum with a moderate spectral resolution. Since the high resolution solar spectrum in the 1300 - 1700 $\dot{A}$ range was taken in 1980 (the solar maximum period of

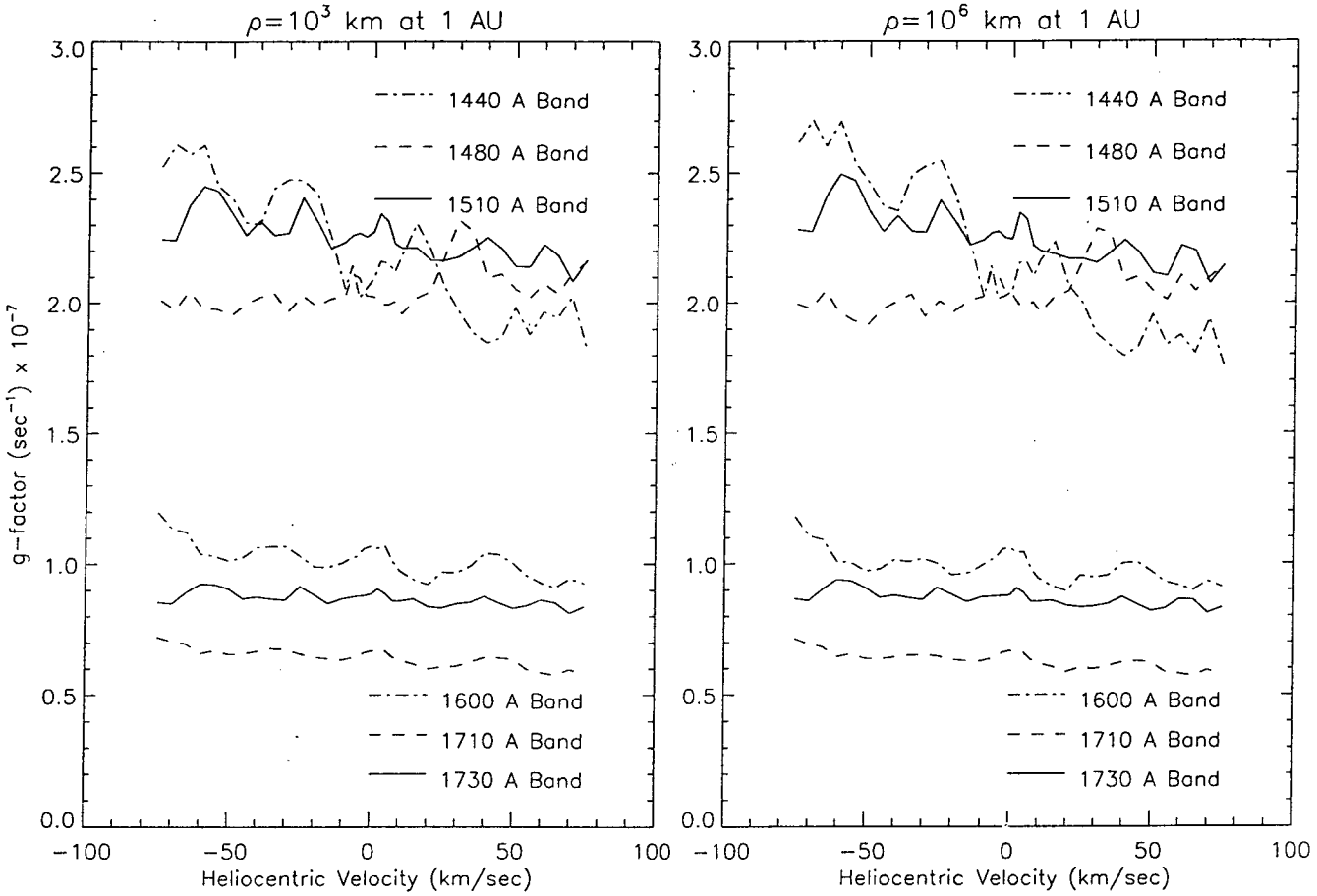

Fig. 8. (a) shows g-factors of 6 bands near 1440, 1480, 1510, 1600, 1710, and 1730 $\dot{A}$ at $\rho = 10^3$ km as a function of heliocentric velocity. As seen in this figure, the g-factors of the bands vary less than 20 velocities. In Figure (b), we present the g-factors of the same 6 bands at $\rho = 10^6$ km.

the cycle 21) and 1984, its intensities in the shorter wavelength region are significantly greater than those of the full-disk spectrum that was taken in 1985 (a quiet sun period). In Figs. 8a and b, for example, the g-factors of the 1510 $\dot{A}$ band (1-0) are between 2×10^{-7} and 2.5×10^{-7}sec^{-1}, whereas the g-factor of the same band in Table 4 is 1.6×10^{-7} sec^{-1}. As we discussed previously, the g-factors in Table 4 are useful for the absolute values of band fluorescence efficiency during the quiet sun period, and Figs. 8a and b are useful for relative g-factor variation as a function of heliocentric velocity. Durrance (1980) derived g-factors for the atmosphere of Venus at a period when the solar activity was relatively high. We scaled the Durrance's value of the 1510 A band to a quiet sun period at 1 AU, and found about 1.8×10^{-7}sec^{-1}, which is approximately in agreement with our value.

IV. CONCLUSION

We have investigated the Swings effects of the A-X system and the fundamental band (v"= 1 → 0) of CO. Our model includes electronic, rotational, and vibrational transitions, excitations by solar UV and infrared radiation, and effects of neutral and electron collisions. We derived fluorescence efficiencies of the bands as functions of heliocentric velocity and cometrocentric distance. We found that the UV Swings effects are less than 20 most bands of the A-X system. We found that neutral collisions are the major process to determine the ground state populations for cometocentric distance less than 10^3 km for a Halley type comet at 1 AU; and electron collisions and infrared excitations for cometocentric distance greater than 10^4 km become the dominant processes to determine the ground

state populations. The significant temporal variation of the solar ultravioet spectrum in the 1200 - 1500 $\dot{A}$ range causes up to 100 oscillator strengths of the UV bands causes about 30 the g-factors. We also found that the solar absorption lines of the fundamental band and hot bands of CO and its isotopes cause a 20 reduction of the g-factor of the fundamental band at heliocentric velocities close to 0 km/sec. We compared a line-by-line model of the A-X system with an IUE spectrum of comet P/Halley and found a satisfactory fit. During the fitting process we found an excessive emission in the 1550 - 1630 $\dot{A}$ range, which may be cometary origin.

APPENDIX

Solar physicists usually obtain high resolution spectra from a small area on the sun. In order to have a full disk spectrum for cometary research, we need to know fractional portions of active and quiet regions along with high resolution spectra from active and quiet regions. The fraction of active regions on the sun is roug

Solar physicists usually obtain high resolution spectra from a small area on the sun. In order to have a full disk spectrum for comentary research, we need to know fractional portions of active and quiet regions along with high resolution spectra from active and quiet regions. The fraction of active regions on the sun is roughly correlated with the plage index and He I 10830 $\dot{A}$ equivalent width. The He line is believed to be the best representing full-disk solar UV activity because the line arises exclusively from chromospheric material and UV radiation from the overlying corona contributes significantly to its formation (e.g., Harvey and Livingston, 1993). Harvey and Livingston decomposed the He line full-disk signal into 4 different components: background, plages, filaments, and coronal holes. They said, "We used daily images mapped into latitude-longitude format. These maps are routinely averaged with weights into single maps of each Carrington rotation. In digital form, a 7-year time series of helium line strengths vs. latitude along the central longitude meridian (6×10^6 values) was convolved with a weighting function that synthesized a daily full-disk average..... It agrees well with the actual daily measurements.....". They noted that the variations of the individual components are principally due to changes in the fractional areas rather than strength variations with the exception of the background component. According to the Fig. 3, in which the 4 components and a summed value are presented, contribution from plages and background ti the He I line with are about 90 holes are about 10 for filaments and coronal holes (and usually we do not have the both spectra), which contribute only 10 we may neglect the both components. Currently the decomposed components are available from the late 1984 to early 1992.

We note another available quiet region spectrum ($\Delta\lambda = 0.07\dot{A}$) in the 1445 - 2100 $\dot{A}$ region (Kjeldseth Moe, et al. 1976), which was taken by a rocket flight. Kjeldseth Moe, et al. also presents an active region (a plage) spectrum with the same spectral resolution in the 1690 - 2100 $\dot{A}$ region. If we know the fractions of quiet regions and active regions on the solar disk at a given time, we can theoretically calculate a high resolution spectrum from 1690 and 2100 $\dot{A}$ using the above spectra. Since the covering range is limited, it is obviously not adequate for the analysis of the A-X band. We may however be able to synthesize a full-disk solar spectrum in the 1690 - 2100 $\dot{A}$ region at a given time between late 1984 to early 1992 using the above decomposed plage and background component indices. High resolution spectra for active and quiet regions in the shorter wavelength range (¡ 1690 $\dot{A}$) are needed.

ACKNOWLEDGEMENTS

We would like to thank Prof. Michael F. A'Hearn for his generous support during the first stage of this research. We are grateful to S. Green for providing the excitationa and deexcitation rates of CO by H_2O collisions. We would also like to thank H. Weaver for pointing out the significant variation of transitions moments of the A-X system as a function of vibrational quantum number, and providing a copy of Durrance's Ph. D. thesis. We would like to acknowledge the efforts of J. Lean and J. Gurman in arranging the solar UV spectra for our study, and M. Geller for the ATMOS solar infrared spectrum. J. Harvey kindly provided us the He I 10830 $\dot{A}$ indices. This work was initiated by a support from NASA Grant NAGW-902, and has been partially supported by a grant from the Korea Science and Engineering Foundation.

REFERENCES

Abdel-Halim, H., and G.E. Ewing 1985. J. Chem. Phys. 82, 5442.
A'Hearn, M.F., J.T. Ohlmacher, and D.G. Schleicher 1983. University of Maryland, Tech. Rep. AP83-044.
Bacic, Z., R. Schinke, and G.H.F. Diercksen 1985. J. Chem. Phys. 82, 236.
Billebaud, F., J. Crovisier, E. Lellouch, T. Encrenaz, and J.P. Maillard 1983. Planet. Space Sci. 39, 213.
Boissoles, J., C. Boulet, D. Robert, and S. Green 1989. J. Chem. Phys. 90, 5392.
Brekke, P. 1993. ApJS, 87, 443
Chandra, N. 1977. Phys. Rev. A. 16, 80.
Chin, G., and H.A. Weaver 1984. ApJ. 285, 858.
Crifo, J.F. 1992.ApJ. 391, 336.
Crovisier, J., and J. Le Bourlot 1983. A&A. 123, 61.
Dickinson, A.S., T.G. Phillips, P.F. Goldsmith, I.C. Percival, and D. Richards 1977. A&A 54, 645.
Disanti, M.A., M.J. Mumma, J.H. Lacy, and P. Parmar 1992. Icarus, 96, 151.
Djeu, N., and S.K. Searles 1972. J. Chem. Phys. 57, 4681.
Durrance, S. T. 1980. Ph. D. thesis. University of Colorado.
Eberhardt, P. et al. 1987. A&A. 187, 481.
Feldman, P.D. 1982, Comets, ed. Wilkening, L.L., Univ. Arizona Press, 461.
Festou, M.C. et al. 1986. Nature, 321, 361.
Harvey, J.W., and W.C. Livingston 1993. Infrared Solar Physics, IAU Sym., Number 154.
Hesser, J.E. 1968. J. Chem. Phys. 48, 2518.
Jain, A., and D.W. Norcross 1992. Phys. Rev. A. 45, 1644.
Kim, S.J., M.F. A'Hearn, and W.D. Cochran 1989. Icarus, 77, 98.
Kjeldseth Moe, O., M.E. VanHoosier, J.-D.F. Bartoe, and G.E. Brueckner 1976. NRL Report 8056, Naval Research Laboratory, Washington, D.C.
Kovác, I. 1969. Rotational Structure in the Spectra of Diatomic Molecules, American Elsevier Pub. Com. Inc. New York.
Lassettre, E.N., and A. Skerbele. 1971. J. Chem. Phys. 54, 1597.
Larsson, M. 1983. A&A. 66, 291.
Lean, J. 1991. Rev. Geophys. 29, 505.
Lee, K.T., and J.M. Bowman 1987. J. Chem. Phys. 86, 215.
Legay-Sommaire, N., and F. Legay 1970. Can. J. Phys. 48, 1966.
Mumma, M.J., E.J. Stone, and E.C. Zipf 1971. J. Chem. Phys. 54, 2627.
Pedersen, A., R. Grard, J.G. Trotignon, C. Beghin, Y. Mikhailov, and M. Mogilevsky 1987. Astron. Astrophys. 187, 297.
Poynter, R.L., and Pickett, H.M. 1992. JPL publication 80-23, Revision 2.
Roux, F., C. Effantin, and J. D'Incan (1972). JQSRT,12, 97-106.
Schleicher, D.G., and M.F. A'Hearn 1982. ApJ. 258, 864.
Schwartz, R.N., Z.I. Slawsky, and K.F. Herzfeld 1952. J. Chem. Phys. 20, 1591.
Tilford, S.G., and J.D. Simmons 1972. J. Phys. Chem. Ref. Data, 1, 147.
Vlahoyannis, Y.P., H. Krueger, and E. Weitz 1987. J. Chem. Phys. 86, 3311.
Weaver, H., P.D. Feldman, M.F. A'Hearn, C. Arpigny, J.B. McPhate, and T.E. Smith 1992. Bull. Amer. Astron. Soc. 24, 992.